Separation Science and Technology
Publication details, including instructions for authors and subscription information:
http://www.informaworld.com/smpp/title~content=t713708471

CROSS-FLOW FILTRATION OF β-LACTOGLOBULIN SOLUTIONS LOADED WITH ADSORBENT PARTICLES

L. Bouzenada[a]; R. Joulié[a]; G. M. Rios[a]; A. Mézaoui[a]
[a] Université Montpellier II—Place E. Bataillon, Montpellier Cedex 5, France

Online publication date: 30 November 2001

To cite this Article Bouzenada, L. , Joulié, R. , Rios, G. M. and Mézaoui, A.(2001) 'CROSS-FLOW FILTRATION OF β-LACTOGLOBULIN SOLUTIONS LOADED WITH ADSORBENT PARTICLES', Separation Science and Technology, 36: 15, 3337 — 3354
To link to this Article: DOI: 10.1081/SS-100107906
URL: http://dx.doi.org/10.1081/SS-100107906

SEPARATION SCIENCE AND TECHNOLOGY, 36(15), 3337–3354 (2001)

CROSS-FLOW FILTRATION OF β-LACTOGLOBULIN SOLUTIONS LOADED WITH ADSORBENT PARTICLES

L. Bouzenada, R. Joulié, G. M. Rios,* and A. Mézaoui

Laboratoire des Matériaux et Procédés Membranaires—
CC 047, Université Montpellier II—Place E. Bataillon,
34095 Montpellier Cedex 5, France

ABSTRACT

The influence of adsorbent particles on the characteristics of protein solution filtration was studied. Three media, activated carbon suspensions, β-lactoglobulin solutions, and a mixture of both, were filtered on a 0.2-μm pore alumina membrane. Moreover, the adsorption of protein on microparticles was studied and 1 isotherm was determined. Comparison of permeate fluxes, apparent retention coefficients, and hydraulic resistance values at steady state conditions highlights the existence of adsorbent-protein interactions. Permeability and retention seems to depend on cross-flow velocity. Correlations are proposed to express steady state fluxes versus operating parameters: cross-flow velocity, transmembrane pressure, and adsorbent and protein concentrations.

Key Words: Cross-flow filtration; Adsorption; Inorganic membrane; β-Lactoglobulin; Activated carbon

*Corresponding author. Fax: +33 4 67 14 91 19; E-mail: rios@iemm.univ-montp2.fr

INTRODUCTION

Cross-flow microfiltration is used extensively in various bioprocesses for such purposes as separation, concentration, purification, sterile filtration, clarification, and wastewater treatment (1). However, the cumulative effects of concentration polarization and fouling, linked to solvent-membrane, solute-membrane, or solute-solute interactions, strongly limit the solvent flux through the membrane (2–4). In fact, the concentration of macromolecular solutes at the membrane surface often causes the precipitation of a gel that further acts as a membrane and offers major resistance to permeate flux.

Considerable research effort has been undertaken to reduce the limiting effect of this hydraulic resistance either by destabilizing the gel layer, through backflushing, electric fields, ultrasonic applications, or pulsated feed flow, or by decreasing its thickness through turbulence promoters, baffles, or rotating surfaces (5). Through the introduction of abrasive particles into the feed solution, the boundary-layer effect can be minimized as can gel thickness (6). By destabilizing the gel layer, both the separation rate and permeate flow of low concentration solutions can be improved through the use of adsorbent particles, which in addition to their erosion effect, reduce the feed concentration and consequently the polarization concentration at the membrane wall. The exploitation of the membrane destabilization as a means of improving separation rate and permeate flow constitutes the principal aim of this work.

The basic study presented here was carried out using two model substances: activated carbon particles and β-lactoglobulin. The former plays a double role of adsorbent and erosion agent, while β-lactoglobulin is the charged organic constituent to be separated from the solvent both by filtration through the membrane and by adsorption on activated carbon. This protein was chosen because of its well-known physical and chemical stability and interest in its industry applications. Activated carbon was selected because of its strong affinity for organic compounds: it is one of the most effective adsorbents currently available for treatment of drinking water and wastewater (7). The filtering element is an asymmetric α-alumina membrane that presents the advantages of high permeability, high resistance to chemical agents and high temperatures, and potential for numerous cycles of reuse after regeneration (8).

Experiments were performed at constant pH and temperature. The permeate flux was recorded at different cross-flow velocities and transmembrane pressures with single adsorbent or protein solutions of various concentrations; data analysis showed the influence of these operating parameters on hydraulic resistance, and retention coefficient values were calculated. In addition, the adsorbent properties of activated carbon toward β-lactoglobulin were determined. The experiments with activated carbon were carried out with the filtration apparatus under hydrodynamic conditions identical to those that characterized the filtration. In the final experiments, mixed solutions incorporating proteins and adsorbent were filtered and a comparison was made between the mixture and the single component solutions.

MARCEL DEKKER, INC.
270 Madison Avenue, New York, New York 10016

MATERIALS AND METHODS

Microfiltration Unit

A schematic diagram of the cross-flow filtration equipment is shown in Fig. 1. A volumetric pump (WANNER, Hydra-Cell) supplies a regular flow directly proportional to the rotation velocity. Past the filtration module, a needle valve allows accurate adjustment of the pressure. A tank equipped with a cooling coil to work in isothermal conditions is used to feed the pump and to collect the retentate and the permeate. A safety valve limits the pressure on the delivery line to prevent damage that could result in the event of a pipe obstruction or over-tightening of the needle valve.

Membrane

The filtering element is an asymmetric tubular membrane made from porous α-alumina (35% porosity) and prepared by Société des Céramiques Techniques. The thickness of the top filtering layer was 40 μm and the mean pore diameter was 0.2 μm. The dimensions of the ceramic support were as follows: 0.23 m in total length and 0.18 m in useful length, o.d. and i.d. values of 19 and 15 mm respectively, and filtering surface area of 8.5×10^{-3} m^2.

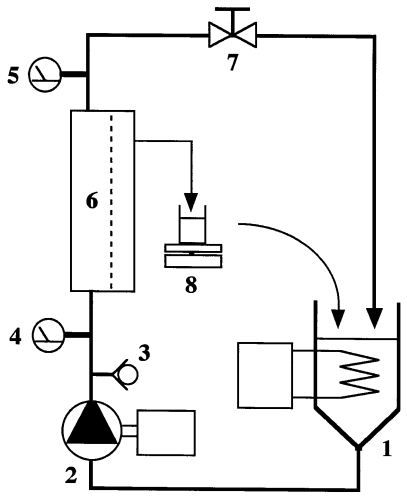

Figure 1. Experimental setup: 1) feeding tank with temperature control, 2) volumetric pump, 3) safety valve, 4 and 5) manometers, 6) filtration module, 7) needle valve, 8) continuous weighting of permeate flow rate.

Chemicals

Ultra-pure water was used as a solvent. Its characteristics at 20°C were as follows: resistivity was higher than 18 MΩ·cm; pH range was 6.5–7.5; maximum residue after evaporation was 0.01 to 0.05 mg/L.

A filtration test with ultra-pure water was performed after each membrane cleaning step so that the correct amounts were recovered from the initial conditions. In the experimental conditions used, the steady state flux of permeate (J_{st}) can be correlated to the pressure drop through the membrane, which is called the transmembrane pressure (Δp), by the following equation:

$$J_{st} = 6.06 \times 10^{-10} \cdot \Delta p \quad (1)$$

in which J_{st} is expressed in m/s and Δp is in Pa.

Activated carbon of the Picazine type was supplied by the PICA Co. It is a macro and micro porous material made from coconut shell and is widely used in processing water. It has an apparent density of 490 kg/m^3 and a BET specific area of 1400 m^2/g.

The particle size distribution, determined using a MALVERN laser diffraction analyzer, highlights a maximum frequency (or mode) of 15 μm and a mean diameter of 22 μm with a standard deviation of 18 μm (Fig. 2). Because the resolution of this analyzer was relatively low (approximately 3 μm at the lower limit), complementary observations were made with an optical microscope. Through the microscope, we found that the smallest particle sizes were greater than 1 μm, which is much higher than the membrane pore diameter of 0.2 μm. Therefore, complete carbon rejection was observed.

β-lactoglobulin is synthesized by the mammary glands of various animals; dairy cows are a primary source of it. It is the most common of the lactic proteins and it constitutes the rich part of milk. The β-lactoglobulin used in this work,

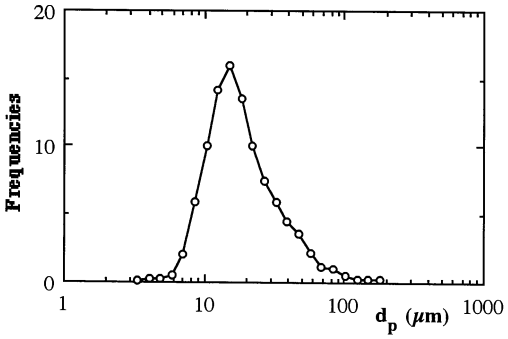

Figure 2. Particle size distribution of activated carbon.

MARCEL DEKKER, INC.
270 Madison Avenue, New York, New York 10016

extracted from lactoserum by chromatographic separation, is of type ALBUVIR 86 NK made by LACTO-BRETAGNE. The isoelectric point is approximately 5.3. β-lactoglobulin molecules are globular with a M.W. 1.836×10^4 g/mol. They join together to form stable dimers at pH values between 6 and 7.

Operating Mode

All the experiments were carried out at a constant temperature of 21 ±1°C.

The permeate flow was measured at regular intervals with an accuracy better than 2.5%. It was then recycled into the feeding tank so that a constant concentration was maintained throughout the process. Between two successive runs, the membrane was cleaned by means of NaOH (2%) and HNO_3 (1%) solutions, at 60°C, and finally rinsed with ultra-pure water until it was at pH = 7.

The protein concentrations in the permeate and the retentate were determined by means of a UV spectrophotometer (UNICAM, 8625) at a wavelength of 280 nm.

The concentration ranges investigated in this study were 0.01 to 5.00 g/L for activated carbon and 1 to 20 g/L for β-lactoglobulin.

Theory

Traditional film-layer theory (9) leads to the well-known expression of permeate flux:

$$J = k \ln\left(\frac{C_m - C_p}{C_f - C_p}\right) \tag{2}$$

where k represents the mass transfer coefficient and C_m, C_p, and C_f are the respective concentrations of solute in contact with the membrane, in the permeate, and in the feed solution.

$$\mathrm{Sh} = a\mathrm{Re}^b\mathrm{Sc}^c \tag{3}$$

from which the following expression, J is deduced:

$$J = \alpha\, U^\beta C_f^\gamma \tag{4}$$

where U is the cross-flow velocity. The coefficients α, β, and γ depend on the flow region and the entrance length of the channel.

In the presence of a cake layer at the membrane surface, the application of Darcy's law gives another form of the expression of permeate flux:

$$J = \frac{1}{A}\frac{dV}{dt} = \frac{\Delta p}{\mu(R_m + R_c)} = \frac{\Delta p}{\mu\, R_t} \tag{5}$$

MARCEL DEKKER, INC.
270 Madison Avenue, New York, New York 10016

where A is the filtering surface area, dV/dt is the permeate flow rate, μ is the permeate viscosity, and R_m, R_c, and R_t are the hydraulic resistances of the membrane, the cake, and the whole system. From the fluxes obtained by filtering pure water and solutions, R_m and R_c may be estimated.

RESULTS

Filtration of Activated Carbon Suspensions

Runs were conducted at 2×10^5 and 4×10^5 Pa (transmembrane pressure) and 0.34, 1.1, and 2.2 m/s (cross-flow velocity). The carbon concentrations, C_{ac}, were fixed at 10, 40, 100, 400, 1000, and 4000 mg/L, and the suspension density remained near that of water. Because the solid-to-liquid volume ratio was considerably lower than 1 (approximately 10^{-3}), a single-phase flow can be assumed (10).

After a short period of cake building, due to particle deposition on the membrane surface, the permeate flow rate quickly approached a constant value. The corresponding steady state flux is always less than that obtained with pure water under the same conditions. The granulometry data of the carbon show that only the presence of a superficial hydraulic resistance can explain the decrease of permeate flux.

Figure 3 shows the variations of permeate flux at steady state as a function of carbon concentration. For concentrations less than 0.1 g/L, flux strongly de-

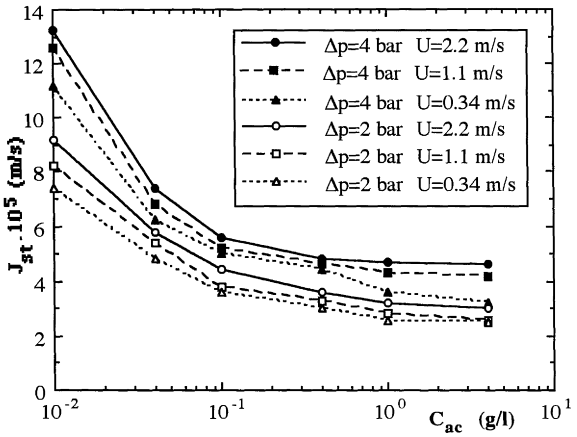

Figure 3. Steady state flux of permeate versus activated carbon concentration: effect of cross-flow velocity and transmembrane pressure.

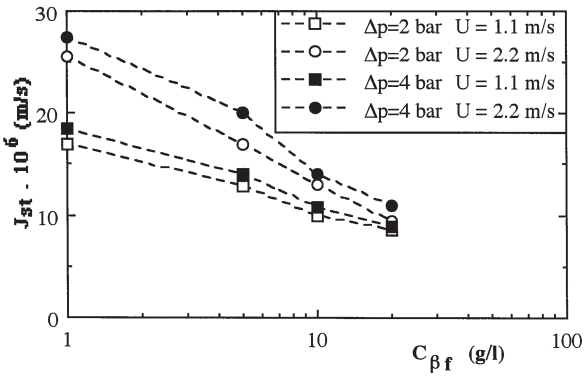

Figure 4. Steady state flux of permeate versus β-lactoglobulin concentration: effect of cross-flow velocity and transmembrane pressure.

clines with increasing concentration. Above 1 g/L, it becomes nearly independent of C_{ac} because the action of shear stresses limits the cake thickness.

Steady state flux also varies with transmembrane pressure and cross-flow velocity. It increases with Δp (especially below 1 g/L) and also more slightly with U (independent of carbon concentration). In the variation ranges of C_{ac}, Δp, and U, the following correlation gives values of J_{st} with a standard deviation of 14% and a maximum gap between experimental and computed values of 25%:

$$J_{st} = 7.67 \times 10^{-8} U^{0.10} C_{\beta f}^{-0.18} \Delta p^{0.49} \tag{6}$$

with J_{st} and U measured in m/s, $C_{\beta f}$ in kg/m^3 (or g/L), and Δp in Pa.

Filtration of β-Lactoglobulin Solutions

β-Lactoglobulin solutions were prepared at 21°C for 24 hours before use. Special attention was paid to avoid development of bacteria. Four concentrations were filtered: 1, 5, 10, and 20 g/L. As usually observed, a significant and rapid drop of permeate flow rate during the first minutes occurred until a stationary plateau was reached. This flow-rate decrease is usually explained by the formation of a polarization layer as well as quick fouling of the membrane due to protein adsorption onto the alumina surface.

Figure 4 shows the variation of steady state fluxes with feed protein concentration $C_{\beta f}$. On one hand, a significant drop of permeate fluxes was observed, and the drop was greater than that obtained for pure water filtration. For example, under $\Delta p = 4 \times 10^5$ Pa and $U = 1.1$ m/s, fluxes can be reduced by a factor 13 for $C_{\beta f} = 1$ g/L and by a factor 27 for $C_{\beta f} = 20$ g/L. On the other hand, J_{st} slightly

increased with cross-flow velocity, but it stayed quasi-independent of transmembrane pressure in the range investigated. These results suggest the setting of a very thin mesh protein, that is a lattice supported by ceramic, that acts as the true filter element. This protein mesh is called the dynamic membrane.

In accordance with Eq. (4), these results can be correlated to U (m/s) and $C_{\beta f}$ (kg/m^3 or g/L) by the following dimensional relationship:

$$J_{st} = 18.8 \times 10^{-6} U^{0.41} C_{\beta f}{}^{-0.276} \tag{7}$$

with J_{st} measured in m/s. The standard deviation and the maximum gap between experimental and computed values are equal to 8.6% and 19.5%, respectively. To take into account the slight effect of transmembrane pressure on steady state flux, a second correlation can also be proposed. In the second correlation Δp is expressed in Pa:

$$J_{st} = 3.4 \times 10^{-6} U^{0.41} C_{\beta f}{}^{-0.276} \Delta p^{0.136} \tag{8}$$

A maximum gap of only 13.8% and a standard deviation of 7.1% is obtained with Eq. (8). Equations (7) and (8) are valid for the ranges: 1.1 m/s $\leq U \leq$ 2.2 m/s; 1 kg/m^3 $\leq C_{\beta f} \leq$ 20 kg/m^3; and 2×10^5 Pa $\leq \Delta p \leq 4 \times 10^5$ Pa.

Hydraulic resistance of the protein layer strongly increased with the increase of both solution concentration and transmembrane pressure; the effect of transmembrane pressure was to compress the layer. Conversely, the increase of cross-flow velocity reduced hydraulic resistance. For example, for $C_{\beta f} = 1$ g/L, R_c is multiplied by a factor 2 when Δp increases from 2×10^5 to 4×10^5 Pa and divided by a factor on the order of 1.5 to 1.7 when U passes from 1.1 to 2.2 m/s. (Values of R_c for $C_{\beta 0} = C_{\beta f}$ are given in Table 1.)

An apparent retention coefficient, $RC = 1 - C_{\beta p}/C_{\beta f}$, is determined in steady-state flux conditions. ($C_{\beta p}$ is the β-lactoglobulin concentration in the permeate.) The variation of RC with protein concentration is presented in Fig. 5. As a rule, the retention coefficient increases with increasing Δp or with decreasing U. Nevertheless, the shape of curves RC vs. $C_{\beta f}$ depends on velocity. At 1.1 m/s, RC regularly declines from about 98% to 93%, whereas RC increases then decreases with increasing $C_{\beta f}$ at 2.2 m/s. This phenomenon, which appears only for $C_{\beta f}$ values below 10 g/L, may result from uncertainty in the accuracy of the measurement of $C_{\beta p}$; it could also be the consequence of an inhomogeneous structure of the dynamic membrane formed at very low protein concentration and high cross-flow velocity.

Adsorption of β-Lactoglobulin onto Activated Carbon

In this appended study, necessary to interpret the filtration of protein-adsorbent mixtures, our aim was to determine kinetics and thermodynamic characteristics of adsorption. Generally, when this type of adsorption is implemented with low fluid-phase concentration, mass transfer is mainly controlled by the degree of

Marcel Dekker, Inc.
270 Madison Avenue, New York, New York 10016

Table 1. Comparison of Results Obtained Filtering Activated Carbon, β-Lactoglobulin, β-Lactoglobulin, and Activated Carbon Mixtures

	Δp (10^{-5}) (Pa)	U (m/s)	J_{st}(10^6) (m/s)	T_r (%)	R_c(10^{-12}) (m^{-1})	R_c/R_t (%)
Activated carbon			38.0	100.0	3.63	69.0
β-Lactobumin	2	1.1	17.0	96.0	10.1	86.0
β-Lactobumin and activated carbon			12.5	90.7	14.35	89.7
Activated carbon			44.0	100.0	3.05	67.0
β-Lactobumin	2	2.2	25.6	87.2	6.16	78.9
β-Lactobumin and activated carbon			16.9	88.6	10.2	86.1
Activated carbon			52.0	100.0	6.06	78.8
β-Lactobumin	4	1.1	18.5	98.0	20.0	92.4
β-Lactobumin and activated carbon			13.5	95.6	28.0	94.4
Activated carbon			56.0	100.0	5.64	79.0
β-Lactobumin	4	2.2	27.5	88.4	12.9	88.7
β-Lactobumin and activated carbon			18.0	94.8	20.6	92.6

$C_{\beta 0}$ = 1 g/L; C_{ac} = 0.1 g/L.

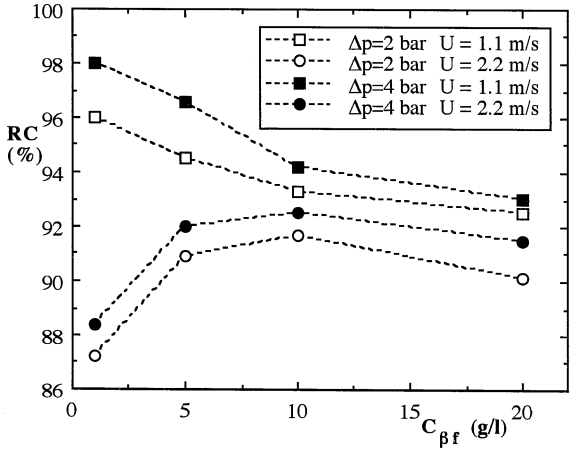

Figure 5. Retention coefficient versus β-lactoglobulin concentration: effect of cross-flow velocity and transmembrane pressure.

mixing produced by the agitation system and by the diffusion of solute from the bulk liquid phase to the external surface of adsorbent particles (11).

For each run, an activated carbon suspension of C_{ac} was added to a β-lactoglobulin solution of initial $C_{\beta 0} = 1$ g/L. This operation was carried out in the filtration apparatus in the absence of transmembrane pressure at a temperature of 21°C. Thus, adsorption takes place under the same experimental conditions as were set during filtration. In all these experiments, the pH was maintained constant by the buffer effect of the protein.

Adsorption Kinetics

The time dependence of the protein concentration in the mixture is important, both to define a minimal contact time and to determine an isotherm. Thus, the β-lactoglobulin concentration, $C_{\beta t}$, was measured at suitable time intervals until a plateau corresponding to the equilibrium concentration $C_{\beta eq}$ was attained. The results, presented in Fig. 6, show an initial rapid decline of concentration during the first minutes. For all carbon concentrations, the plateau was reached after approximately 40 minutes.

Adsorption Isotherm

The isotherm curve is determined from the equilibrium concentration values. The adsorbed mass of β-lactoglobulin (m_β) per unit mass of activated carbon

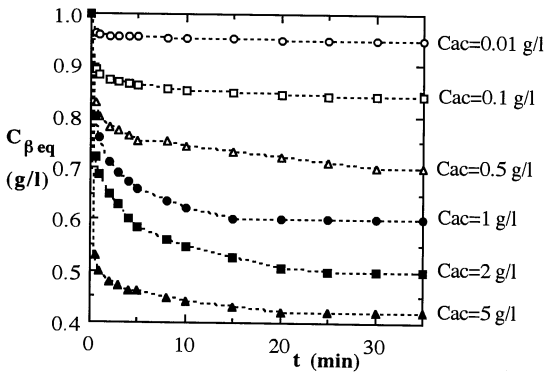

Figure 6. Variation of protein concentration versus time: effect of adsorbent concentration.

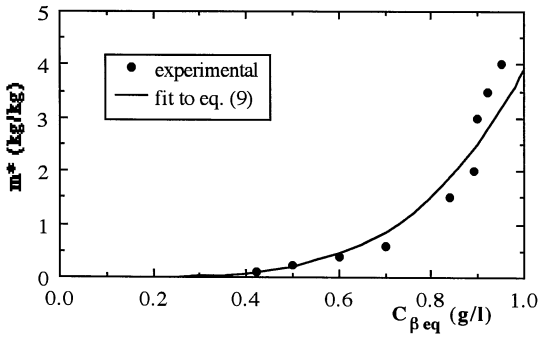

Figure 7. Adsorption isotherm at 21°C ($C_{\beta 0}$ = 1 g/L).

(m_{ac}), $m^* = m_\beta/m_{ac}$, is plotted vs. $C_{\beta eq}$ in Fig. 7. The convex shape of the curve, of type III in the BET classification, means that attraction between adsorbed molecules is strong compared to the attraction of adsorbents to adsorbates (12). Among numerous models, the Freundlich equation

$$m^* = K_F C_{eq}^{n_F} \tag{9}$$

gives a good fit. This result is frequently encountered with activated carbon, which is macroporous and presents a heterogeneous surface. A least-squares analysis provides the Freundlich coefficients, with a correlation coefficient of 0.98, as follows: $K_F = 3.92$ and $n_F = 4.23$.

The equilibrium concentration versus the carbon concentration is plotted in Fig. 8. The protein concentration in the feed flow at the time of mixture filtration can be determined from this curve as $C_{\beta 0}$ is still equal to 1 g/L.

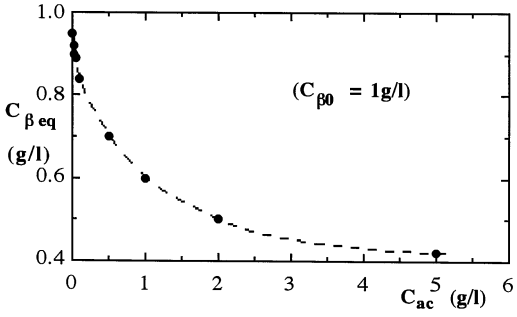

Figure 8. Protein concentration versus activated carbon concentration.

Filtration of β-Lactoglobulin–Activated Carbon Mixtures

Solutions were prepared in the pilot plant apparatus. To prevent the convection of any parasite species toward the membrane, the following procedure was conducted. A carbon suspension was first circulated into the filtration apparatus without transmembrane pressure. Then, a suitable volume of β-lactoglobulin solution was added. After mixing the solutions, the operating pressure was established. The amount of protein adsorbed on the membrane was considered very low compared to that fixed on the carbon because of the large surface area difference of the two solid phases. The contents of the mixtures were as follows: 1 g/L of β-lactoglobulin and 0.01, 0.04, 0.1, 0.5, 1, 2, and 5 g/L of activated carbon.

Figure 9 shows the variation of the steady state flux of permeate with carbon concentration for various velocity-pressure values. A rapid decrease of J_{st} was observed as long as carbon concentration was lower than approximately 1 g/L. J_{st} seems to be insensitive to higher C_{ac}. However, the flux increased with increasing U and Δp. The following dimensional correlation is established between steady state flux and operating parameters:

$$J_{st} = 2.84 \times 10^{-6} U^{0.4} C_{ac}^{-0.05} \Delta p^{0.11} \tag{10}$$

with J_{st} and U measured in m/s, C_{ac} in kg/m^3 (or in g/L), and Δp in Pa. Values estimated through this equation have a standard deviation of 3.9% and a maximal deviation of 10.4% compared to measured values. The validity of Eq. (10) is limited to the ranges: $C_{\beta 0} = 1$ g/L; 0.01 g/L $\leq C_{ac} \leq 5$ g/L; 1.1 m/s $\leq U \leq 2.2$ m/s; 2×10^5 Pa $\leq \Delta p \leq 4 \times 10^5$ Pa.

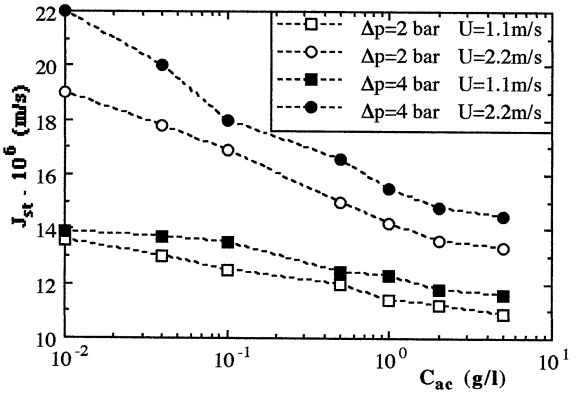

Figure 9. Steady state flux of permeate versus activated carbon concentration: effect of cross-flow velocity and transmembrane pressure.

MARCEL DEKKER, INC.
270 Madison Avenue, New York, New York 10016

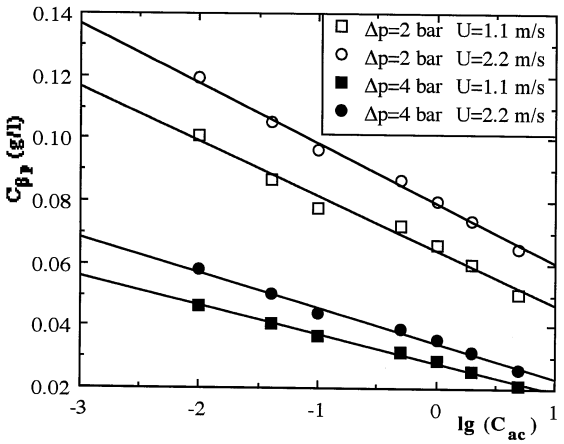

Figure 10. β-Lactoglobulin concentration in the permeate versus logarithm of activated carbon concentration: effect of cross-flow velocity and transmembrane pressure.

The β-lactoglobulin concentration in the permeate ($C_{\beta p}$) versus activated carbon concentration (C_{ac}) is presented in Fig. 10. On one hand, these curves show that an increase of pressure strongly reduces the passage of protein molecules through the membrane, which is an opposite effect from that obtained with increasing velocity. On the other hand, for each velocity-pressure pair, the diagram highlights a linear variation of $C_{\beta p}$ as a function of log (C_{ac}):

$$C_{\beta p} = a + b \log (C_{ac}) \tag{11}$$

in which the coefficients a and b depend on U and Δp. A multiregression analysis gives the following correlation:

$$C_{\beta p} = 1.26 \times 10^{-5} U^{0.3}\, \Delta p^{-1.19} - 492 U^{0.217}\, \Delta p^{-0.84} \log(C_{ac}) \tag{12}$$

with $C_{\beta p}$ and C_{ac} measured in kg/m^3 (or in g/L), U in m/s, and Δp in Pa. In the range of the investigation defined above, this equation fits very well with a standard deviation of 2.5% and a maximal deviation of 5.1%.

Two sets of curves showing the apparent retention coefficient versus carbon concentration are plotted in Fig. 11. In the first set of data (dotted lines), the values of *RC* were calculated with the initial value $C_{\beta 0}$ for feed concentration. The second data set (continuous lines), which is more realistic, was calculated based on the equilibrium concentration $C_{\beta eq}$ obtained after adsorption ($C_{\beta eq} \equiv C_{\beta f}$). In both cases, a better retention was obtained at lower velocity and, in particular, at higher pressure. *RC* increases by about 5 or 6% when Δp varies from 2×10^5 to 4×10^5 Pa. However, the effect of carbon concentration on retention coefficient was negligible, with a maximum retention noted for approximately 0.1 g/L of activated car-

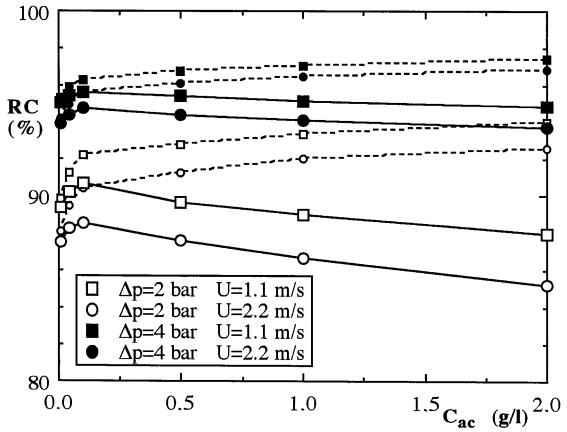

Figure 11. Retention coefficient versus activated carbon concentration: effect of cross-flow velocity and transmembrane pressure.

bon. This phenomenon could be explained by the characteristics of the dynamic membrane. When the adsorbent concentration increases from zero, carbon particles, loaded and wrapped in proteins, form a less permeable layer than does the protein gel alone. When the carbon concentration becomes sufficiently high, the dynamic membrane is far less structured and filtration is mainly controlled by particle cake. The limiting value of 0.1 g/L of activated carbon and the protein deposits are components of an explanation that are in good agreement with the evidence previously discussed regarding filtration of single adsorbent or protein solutions.

Table 2 sums up the general trend of quantities J_{st}, RC, R_c, and $C_{\beta p}$ as a function of U, Δp, and C_{ac}. A logical trend appears with increasing U and Δp: J_{st} increases in all cases; RC and R_c decrease with U (shear stress effect) but significantly increase with Δp (compression of layer); conversely, $C_{\beta p}$ increases with U

Table 2. Summary of Flux, Retention Coefficient, Hydraulic Resistance, and Permeate Concentration Trends with Increased Cross-Flow Velocity, Transmembrane Pressure, and Carbon Concentration

	U ↗	Δp ↗	C_{ac} ↗
J_{st}	↗	↗	↘
T_r	↘	↗↗	~
R_c	↘	↗↗	↗↗
$C_{\beta p}$	↗	↘	↘

↗ increase, ↘ decrease, ~ low variation

MARCEL DEKKER, INC.
270 Madison Avenue, New York, New York 10016

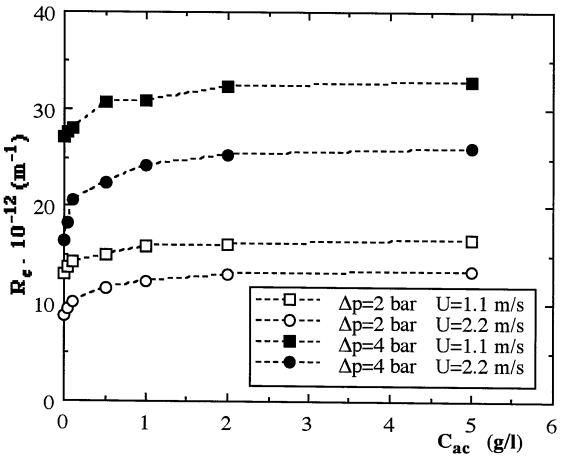

Figure 12. Hydraulic resistance of dynamic membrane versus activated carbon concentration: effect of cross-flow velocity and transmembrane pressure.

and decreases with Δp. More adsorbent particles reduce the flux and the permeate concentration, and increase resistance at the wall; variation of *RC* remains low.

The presence of adsorbent slightly improves retention at approximately 0.1 g/L of activated carbon, but it does not bring the expected improvement for the flux. As shown in Fig. 12, the increase of cake resistance with increasing C_{ac} can reach 25 to 55%.

CONCLUSION

To compare the filtration characteristics of activated carbon suspensions, β-lactoglobulin solutions and β-lactoglobulin–activated carbon mixtures, results obtained in similar operating conditions and for 1 g/L of protein and 0.1 g/L of carbon are shown in Table 1. For each system, the steady state flux increases with increasing U and Δp. The retention coefficient, constant for an activated carbon suspension, decreases with U and increases with Δp for the two other fluids. In all cases, *RC* remained between 87 and 100%. Similar variations were observed for the cake−gel layer resistance, as well as for R_c/R_t, except for the case of an activated carbon suspension for which R_c/R_t seems to be independent of U.

The effects of the presence of activated carbon in protein solution are the following:

decrease of steady state flux and consequent increase of hydraulic resistance;
increase of R_c/R_t;

decrease for $U = 1.1$ m/s and increase for $U = 2.2$ m/s of retention coefficient.

These results lead to the conclusion that, on one hand, adsorbent particles are surrounded by a protein layer that reduces their efficiency as erosion agents, and on the other hand, that the activated carbon plays a binder role within the dynamic membrane.

A consequent reduction of permeability toward solvent and a certain compressibility of the dynamic membrane are apparent. Retention of solute seems to depend on cross-flow velocity.

NOMENCLATURE

A	filtering surface area (m^3)
a, b, c	coefficients (–)
C_{ac}	activated carbon concentration (kg/m^3)
C_f	concentration of solute in the bulk feed (kg/m^3)
C_p	concentration of solute in the permeate (kg/m^3)
C_m	concentration of solute at the membrane surface (kg/m^3)
$C_{\beta eq}$	equilibrium concentration of β-lactoglobulin in solution (kg/m^3)
$C_{\beta f}$	β-lactoglobulin concentration in the feed (kg/m^3)
$C_{\beta p}$	β-lactoglobulin concentration in permeate (kg/m^3)
$C_{\beta t}$	β-lactoglobulin concentration in solution at time t (kg/m^3)
$C_{\beta 0}$	initial β-lactoglobulin concentration in solution (kg/m^3)
D	molecular diffusion coefficient (m^2/s)
d_h	hydraulic diameter (m)
d_p	particle size (μm)
J	volumetric flux through membrane ($m^3/m^2 \cdot s$ or $m \cdot s$)
J_{St}	steady state flux through membrane ($m^3/m^2 \cdot s$ or m/s)
K_F	Freundlich constant $(kg/kg(m^3/kg)^{n_F}$
k	mass transfer coefficient (m/s)
m_{ac}	mass of activated carbon (kg)
m_β	mass of adsorbed β-lactoglobulin (kg)
m^*	amount adsorbed per unit weight of carbon (kg/kg)
n_F	Freundlich factor (–)
RC	apparent retention coefficient (–)
R_c	hydraulic resistance of the cake (or gel layer) (m^{-1})
R_m	hydraulic resistance of membrane (m^{-1})
R_t	total hydraulic resistance (m^{-1})
Re	Reynolds number $\left(\mathrm{Re} = \frac{\rho U d_h}{\mu}\right)$(–)

MARCEL DEKKER, INC.
270 Madison Avenue, New York, New York 10016

Sc	Schmidt number $\left(\mathrm{Sc} = \frac{\mu}{\rho D}\right)$(–)
Sh	Sherwood number $\left(\mathrm{Sh} = \frac{k\, d_h}{D}\right)$(–)
t	time (s)
U	cross-flow velocity (m/s)
V	volume (m^3)
α, β, γ	coefficient (–)
Δp	transmembrane pressure difference (Pa)
μ	dynamic viscosity (Pa/s)
ρ	density of fluids (kg/m^3)

REFERENCES

1. Belfort, G.; Davis, R.H.; Zydney, L. The Behaviour of Suspensions and Macromolecular Solutions in Crossflow Microfiltration. J. Memb. Sci. **1994,** *96*, 1–58.
2. Tarleton, E.S.; Wakeman, R.J. Understanding Flux Decline in Crossflow Microfiltration. Part II. Effects of Process Parameters. Trans. I. Chem. Eng. **1994,** *72*, 431–440.
3. Carrère, H.; René, F. Effet des Paramètres Opératoires sur les Performances des Procédés de Micro-et Ultrafiltration. Entropie **1996,** *197*, 17–32. (in French)
4. Clark, W.M.; Bansal, A.; Sontakke, M.; Ma, Y.H. Protein Adsorption and Fouling in Ceramic Ultrafiltration Membranes. J. Memb. Sci. **1991,** *55*, 21–38.
5. Holdich, R.G.; Zhang, G.M. Crossflow Microfiltration Incorporating Rotational Fluid Flow. Part A. Trans IChemE. **1992,** *70*, 527–536.
6. Milisic, V.; Bersillon, J.L. Antifouling Techniques in Cross-Flow Microfiltration. Filtr. Separat. **1986,** *23* (6), 347–350.
7. Chatzopoulos, D.; Varma, A. Activated Carbon Adsorption and Desorption of Toluene in the Aqueous Phase. AIChE J. **1993,** *39* (12), 2027–2041.
8. Pradános, P.; Arribas, J.I.; Hernández, A. Retention of Proteins in Cross-Flow UF Through Asymmetric Inorganic Membranes. AIChE J. **1994,** *40* (11), 1901–1910.
9. Nakao, S.; Nomura, T.; Kimura, S. Characteristics of Macromolecular Gel Layer formed on Ultrafiltration Tubular Membrane. AIChE J. **1979,** *25* (11), 615–622.
10. Fortier, A. *Mécanismes des suspensions*. Masson: Paris, 1976; 17–33. (in French)

MARCEL DEKKER, INC.
270 Madison Avenue, New York, New York 10016

11. McKay, G.; El Geundi, M.; Nassar, M.M. External Mass Transport Processes during the Adsorption of Dyes onto Bagasse Pith. Water Res. **1988,** *22* (12), 1527–1533.
12. Kovach, J.L. Gas-Phase Adsorption and Air Purification. In *Carbon Adsorption Handbook*; Cheremisinoff, P.N., Ellerbusch, F., Eds.; Ann Arbor Science: Ann Arbor, Mich, 1978; 336–338.

Received October 2000
Revised January 2001

Request Permission or Order Reprints Instantly!